

Markus Vennebusch, Steffen Schön

Institut für Erdmessung, Leibniz Universität Hannover, Germany, eMail: vennebusch@ife.uni-hannover.de

Introduction:

Atmospheric turbulence induces physical correlations on any space geodetic technique based on electromagnetic waves. Thus, also GNSS phase observations are both temporally and spatially correlated due to refractivity fluctuations along the signal's path from the transmitter to the receiver. Currently, these physical correlations are rarely considered in GNSS data analysis; yielding too optimistic parameter variances and covariances.

Based on turbulence theory, Schön and Brunner (2008) developed a formulation of the variances and covariances induced by refractivity fluctuations in the troposphere. This model adequately describes the variance-covariance matrix (VCM) of tropospheric slant delays. The parametrisation is mainly based on the turbulence structure constant, the outer scale length, the integration height, the wind direction and the observation geometry.

The VCM can adequately be used to determine synthetic slant delay time series. In this poster, this strategy is described by using an exemplary GPS configuration. Furthermore, the latest results of simulation studies and sensitivity analyses of this VCM model with respect to the model parameters are presented. As a result, the most dominant parameters (that should be either determined with special care or precisely known) are identified.

Stochastic modelling of atmospheric fluctuations:

The stochastic model of GNSS phase observations developed by Schön and Brunner (2008) uses the von Karman spectrum of refractivity fluctuations to model the covariance $\langle \phi_A^i, \phi_B^j \rangle$ of two carrier-phase observations performed at two stations A and B to two satellites i and j as

$$\langle \phi_A^i, \phi_B^j \rangle = \frac{12.033 \sqrt{\pi^3} \kappa_0^{-2} 2^{-\frac{1}{3}}}{5 \Gamma(\frac{5}{6}) \sin \varepsilon_A^i \sin \varepsilon_B^j} C_n^2 \times \int_0^H \int_0^H (\kappa_0 d)^{\frac{1}{3}} K_{-\frac{1}{3}}(\kappa_0 d) dz_1 dz_2 \quad (1)$$

with Γ denoting the Gamma function and K the modified Bessel function of second kind; also called MacDonald function. The variables and their values as used for the following investigations are summarised in Table 1. Eq. (1) must be evaluated numerically. Since the carrier phase variations are caused by tropospheric refractivity fluctuations the VCM derived by Eq. (1) also describes the stochastic behaviour of slant tropospheric delays and thus enables simulations as described below. Figures 2 and 3 show example correlation matrices derived from VCMs computed by Eq. (1). The decorrelating effect of wind can clearly be recognized.

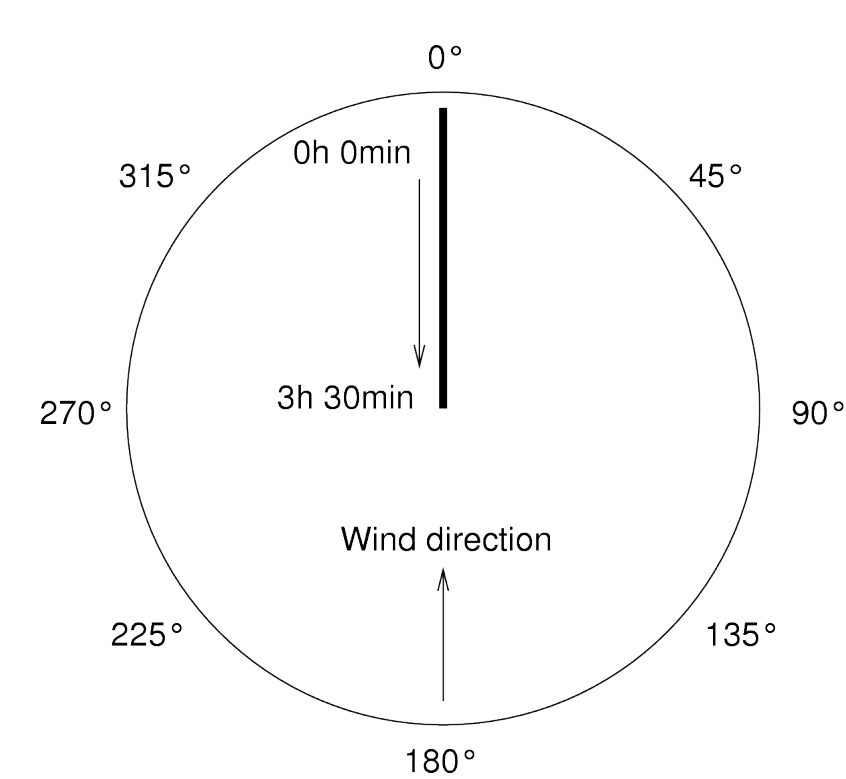


Figure 1: Sky plot of artificial satellite geometry used for investigations: A single satellite rises at 0° azimuth from 3° to 90° elevation within 3.5 hours.

Variable:	Value (and/or unit):	Description:
C_n^2	$1.2e-9 [m^{-20}]$	Structure constant of refractivity
$k_0 = 2\pi/L_0 = 2\pi/6000$	$2\pi/6000 [1/m]$	Wave number to corresponding outer scale length L_0
$a=b=c$	1 [-]	Elongations of turbulent structures (a, b: horizontal, c: vertical)
ε_A^i	3 - 90 [°]	Elevation of satellite i at station A
v_0	0.5 [m/s]	Wind velocity
α_w	180 [°]	Wind direction (azimuth)
ε_w	0 [°]	Wind direction (elevation)
H	1000 [m]	Height of wet troposphere (integration height)
d	[m]	separation distance between the actual integration points

Table 1: Parameter values as used in sensitivity analyses and slant delay turbulence simulations (unless otherwise stated)

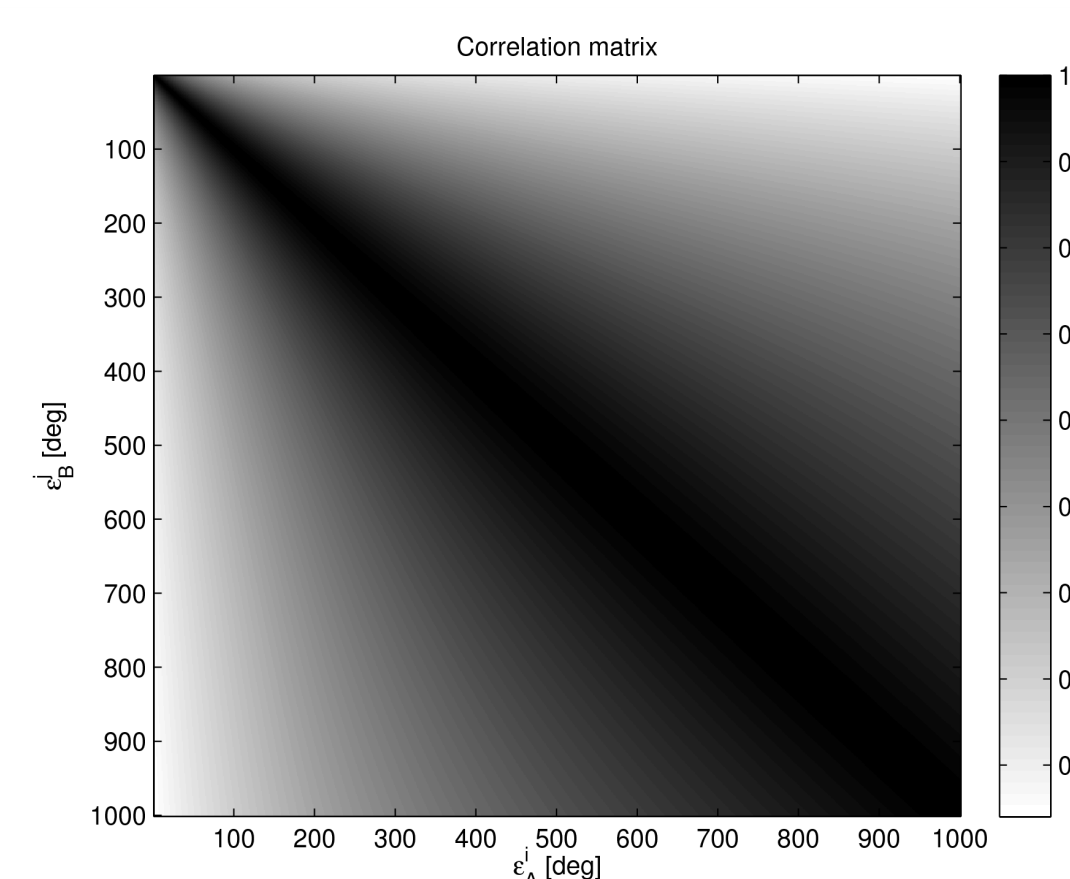


Figure 2: Example correlation matrix ($C_n^2 = 1.0e-7 [m^{-12}]$, wind velocity = 0.0 [m/s])

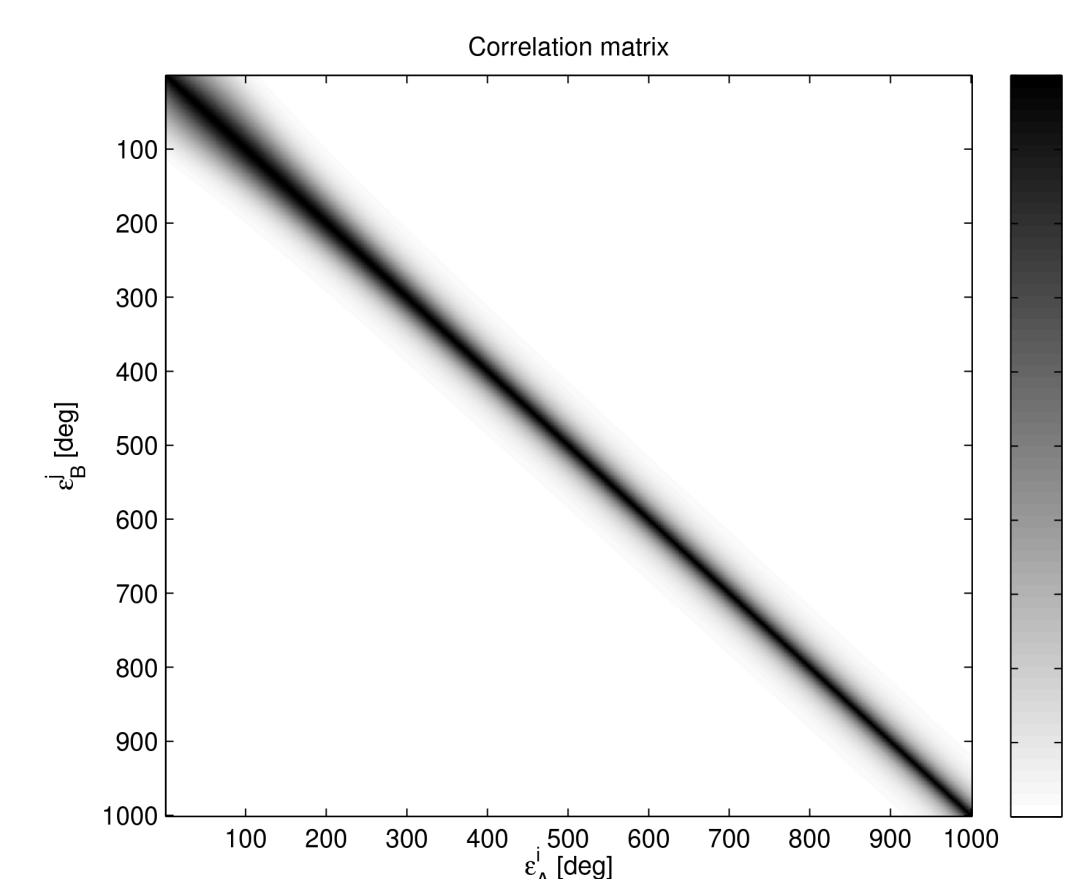


Figure 3: Example correlation matrix ($C_n^2 = 1.0e-7 [m^{-12}]$, wind velocity = 4.0 [m/s])

Sensitivity analysis:

In order to identify the most influential parameters of a model (and thus the parameters which either have to be determined with special care or which have to be precisely known) the total differential of Eq. (1) is used. The general definition of a total differential reads

$$df(x_1, x_2, \dots, x_n) = \sum_{i=1}^n \frac{\partial}{\partial x_i} f(x_1, x_2, \dots, x_n) dx_i = \sum_{i=1}^n f_{x_i} dx_i$$

and has been applied to Eq. (1). Terms with large prefactors f_{x_i} are thus considered as of high impact on the covariance $\langle \phi_A^i, \phi_B^j \rangle$. Since Eq. (1) contains a double integral the following theorem is used

$$\frac{d}{dy} \int_a^b f(x, y) dx = \int_a^b \frac{\partial f(x, y)}{\partial y} dx$$

which shows that differentiation and integration can be exchanged if the integral over $f(x, y)$ is defined, if $f(x, y)$ is continuous and if the partial derivative of $f(x, y)$ with respect to y exists. For Eq. (1) these requirements are fulfilled.

As an example, Figure 4 shows the partial derivative of Eq. (1) with respect to C_n^2 for a fixed observation geometry with two simultaneous observations at 25° and 50° elevation (azimuth 0°, the remaining parameter values are shown in Table 1). The double integral of this function (i.e., the volume below the surface shown in Figure 4) indicates the impact of small variations of C_n^2 on the covariance $\langle \phi_A^i, \phi_B^j \rangle$. Table 2 shows the relation of the double integral values of the respective partial derivatives of Eq. (1) with respect to the most important model parameters. Thus, for the example geometry of two observations at 25° and 50° elevation variations of the turbulence parameters outer scale length L_0 (or the corresponding wave number k_0) and structure constant C_n^2 have the largest impact and show that these parameters should thus be known most precisely (see also Table 2).

Parameter:	k_0	C_n^2	a	c	ε_A^i	v	b	α_w
Double integral value:	-0.093	0.045	0.034	0.015	-0.009	0.00001	0.0	0.0

Table 2: Double integral values of partial derivatives of Eq. (1) wrt main model parameters for two simultaneous observations at 25° and 50° in the example observation geometry.

For a more general investigation the double integral values for all elevation combinations (in 5° steps from 5° to 90° elevation) have been computed and displayed in Figures 5 to 7 for the two main parameters C_n^2 and k_0 . Again, the most influential parameters are k_0 and C_n^2 , especially when both observations are performed at low elevations. Figure 5 and Table 3 show that small variations of C_n^2 lead to small positive covariance variations. On the other hand, small variations of k_0 cause negative variations of the covariance (with a similar (absolute) effect as variations of C_n^2), see Figure 6. Figure 7 shows that a different L_0 value (changed from $L_0=6000$ [km] in Fig. 6 to $L_0=12000$ [km] in Fig. 7) acts as a scaling. The average impact of the remaining parameters on the covariance is shown in Table 3.

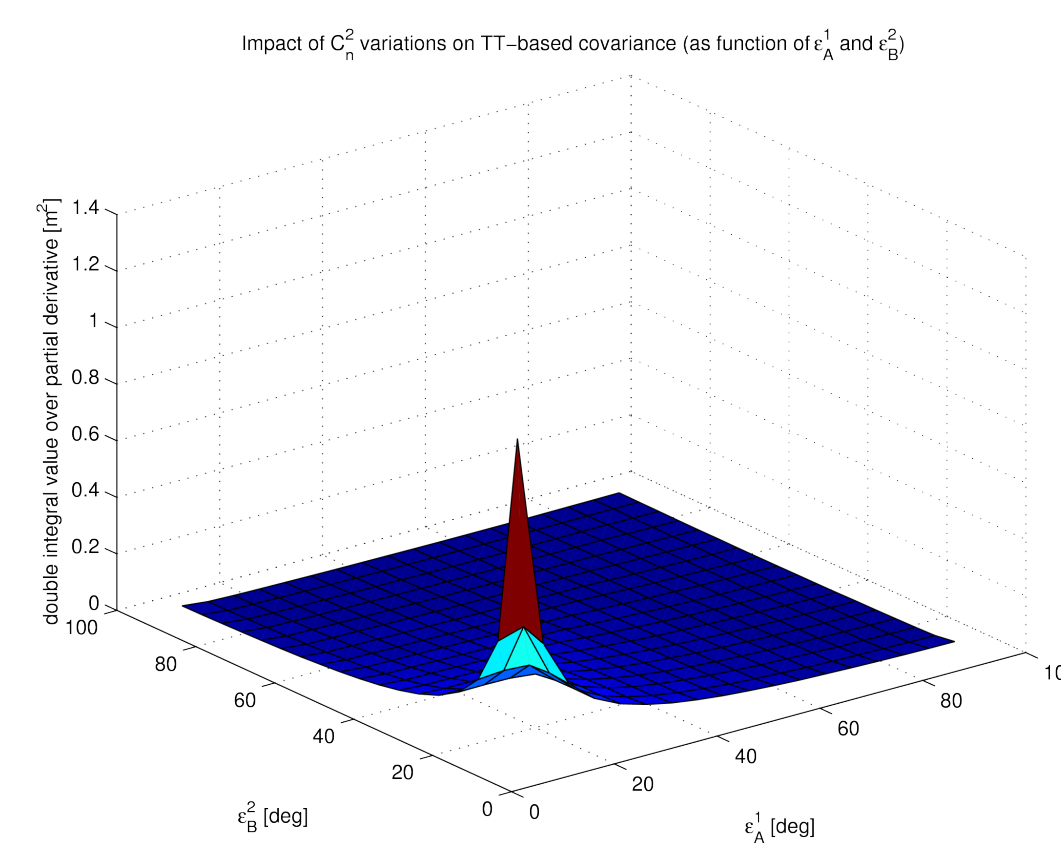


Figure 5: Double integral values of the partial derivative of Eq. (1) wrt C_n^2 (and thus prefactors in the total differential of Eq. (1)).

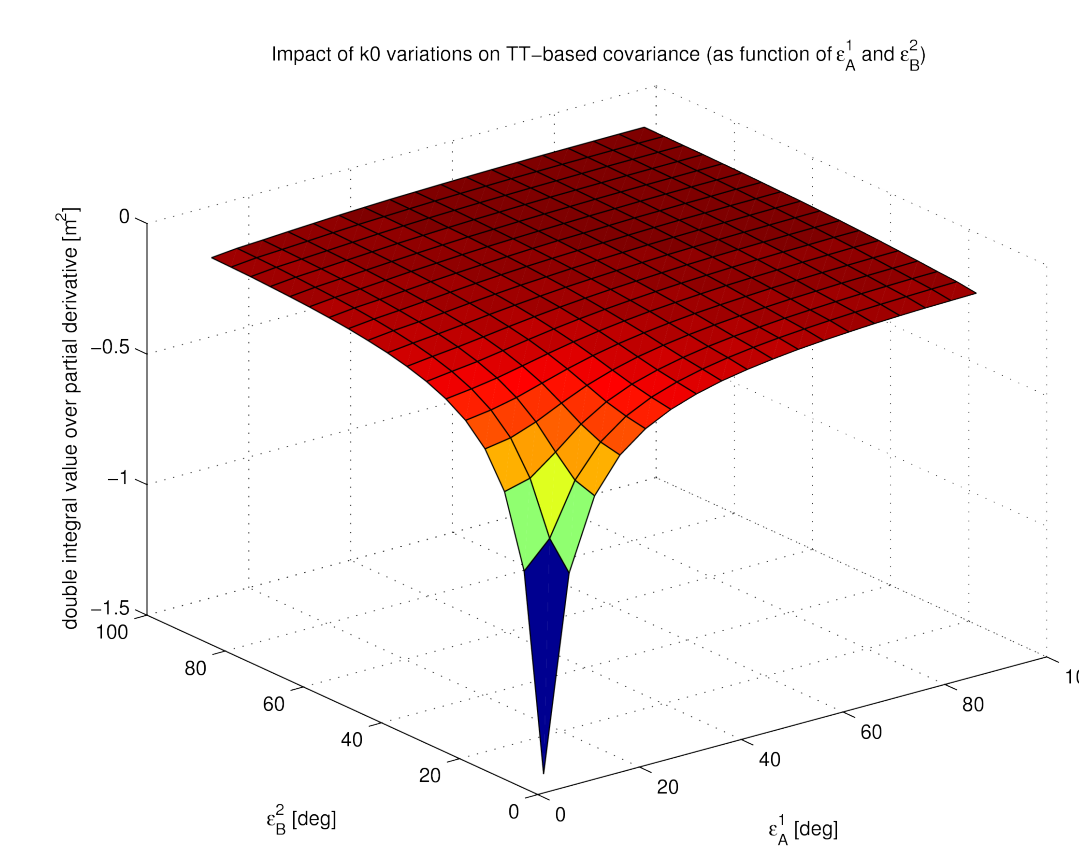


Figure 6: Double integral values of the partial derivative of Eq. (1) wrt k_0 (and thus prefactors in the total differential of Eq. (1)) with $L_0=6000$ [km].

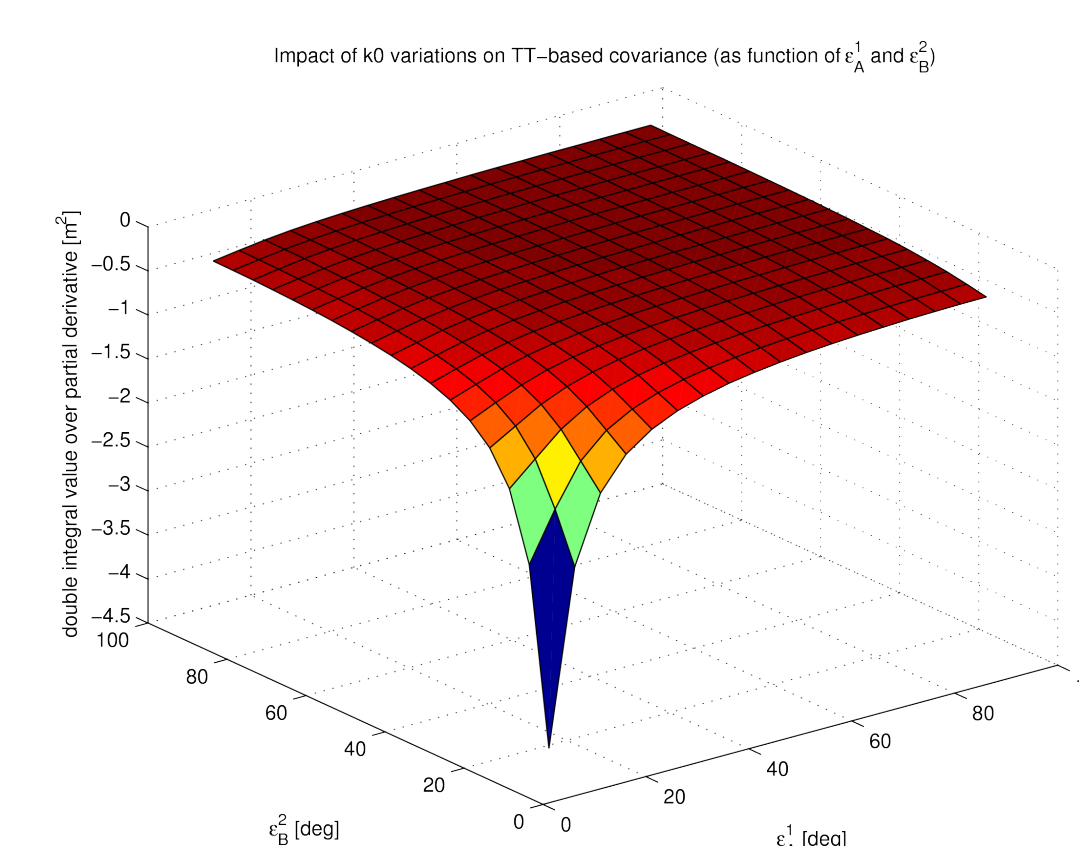


Figure 7: Double integral values of the partial derivative of Eq. (1) wrt k_0 (and thus prefactors in the total differential of Eq. (1)) with $L_0=12000$ [km].

Parameter:	k_0	C_n^2	ε_A^i	c	a	v	b	α_w
Double integral value:	-0.038	0.035	-0.034	0.015	0.00003	0.00001	0.0	0.0

Table 3: Average double integral values of partial derivatives of Eq. (1) wrt main model parameters for all possible observations in the example observation geometry.

Conclusions:

The analysis of the double integral values of the partial derivatives (i.e., the terms of the total differential) of Eq. (1) for an exemplary observation geometry showed that covariance variations are mainly caused by variations of the turbulence parameters k_0 and C_n^2 . Hence, these parameters need to be specified most precisely. On the other hand, some parameters are of negligible impact. Obviously, these results are only valid for the artificial observation geometry shown in Figure 1. Further investigations will concentrate on more general observation geometries.

Simulation of slant delay turbulence:

A variance-covariance matrix Σ_{yy} derived from Eq. (1) can be used to simulate the turbulence of a slant delay time series y . In general, a time series y with predetermined stochastic properties Σ_{yy} can be obtained by a transformation

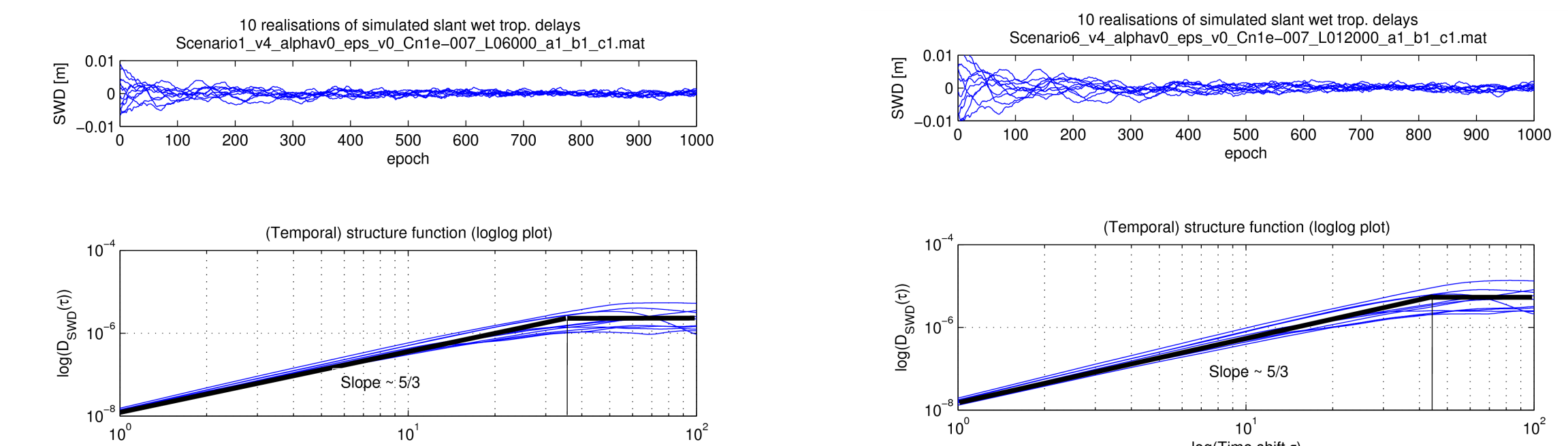
$$y = Wx$$

with x being a Gaussian random vector with $x \sim N(0, 1)$ and a transformation matrix W . Since

$$\Sigma_{yy} = W \Sigma_{xx} W' = W W'$$

and with the Cholesky-decomposed variance-covariance matrix $\Sigma_{yy} = Q' Q$ the transformation matrix W reads: $W = Q'$.

Figures 8 and 9 show several realisations of synthetic slant delays generated by using a 1000×1000 VCM for the example geometry (see Figure 1) with different values for the outer scale length L_0 (but the same values for C_n^2). The sampling rate of the simulated observations is 11.6 seconds (due to an assumed constant rising velocity of the satellite). Larger variations can be seen for larger values of the outer scale length L_0 .



Figures 8 and 9: Simulated turbulence of slant wet tropospheric delays ($C_n^2 = 1.0e-7 [m^{-12}]$, left: $L_0=6000$ [km], right: $L_0=12000$ [km]) and loglog-plots of the corresponding temporal structure functions.

The lower part of the plots shows the structure functions of the generated times series. In general, a structure function is defined by

$$D_{SD}(\tau) = \langle [SD(t+\tau) - SD(t)]^2 \rangle$$

The loglog-plots of the temporal structure functions show a power law behaviour of the generated time series, i.e.

$$D_{SD}(\tau) = C_n^2 \tau^\alpha \quad (2)$$

The slopes of the respective adjusting straight lines (and thus the exponent α of Eq. (2)) are approximately 5/3. This indicates a three-dimensional turbulence process (i.e., station separation small compared to the tropospheric height) and was expected since the model given by Eq. (1) is based on a von Karman spectrum with an exponent of -11/3. In addition, the larger value of the outer scale length L_0 leads to a larger value of the time shift where the structure function approaches a constant value (saturation point).

Outlook:

In future, the current sensitivity investigations will be extended to both more complex and more realistic observation geometries. The simulation of slant wet delay turbulence will also be extended and simulated time series will be compared to results obtained from real data. Future investigations will especially focus on the relation of e.g. outer scale length and saturation points of simulated and real SWD time series.

References:

- Gradinarsky LP: Sensing atmospheric water vapor using radio waves. Dept. Radio and Space Science, School of Electrical Engineering, Chalmers University of Technology, Göteborg, 2002.
- Nilsson T, Haas R, Elgered G: Simulations of Atmospheric Path Delays Using Turbulence Models, Proc. of the 18th Working Meeting on European VLBI, TU Vienna, 2007.
- Schön S, Brunner FK: Atmospheric turbulence theory applied to GPS carrier-phase data, J Geod 82: 47-57, 2008.
- Wheeler AD: Electromagnetic scintillation-I. Geometrical optics. Cambridge University Press, Cambridge, 2001.

Acknowledgements:

This research is funded by Deutsche Forschungsgemeinschaft (DFG, German Research Foundation) through the research grant SCHO 1314/1-1.